Proceedings of the Second International Conference on Press-in Engineering 2021, Kochi, Japan – Matsumoto et al (eds)

Reliability analysis on cantilever retaining walls embedded into stiff ground (Part 2: Construction management with piling data)

N. Suzuki
GIKEN LTD., Tokyo, Japan

Y. Ishihara
GIKEN LTD., Tokyo, Japan

K. Nagai
The University of Tokyo, Tokyo, Japan

ABSTRACT: Part 1 showed that the scatters of the depth influenced the rotational and deformation failure of the cantilever retaining wall, especially when it is embedded short into stiff ground. This part considers on how to deal with the uncertainty using the piling data. Reliability and cost analyses draw following conclusions. The effect of the piling data on the expected total cost are about 8% for Serviceability Limit State and 27% for Ultimate Limit State at most. The construction management with the piling data has advantages especially when the uncertainty of the depth of the rock layer surface are large and additional geotechnical investigations are conducted, and when embedment depth is short. Furthermore, with the piling data, the expected total cost becomes less susceptible to the scatters of the depth of the rock layer surface, which make the proposed method effective in practice.

1 INSTRUCTIONS

1.1 *Part 1*

The reliability analysis of Part 1 (Suzuki et al. 2021) found that the contribution of the scatters of the depth of the rock layer surface to the rotational and deformation failure of the cantilever walls was large.

In the case of pile foundations, it has been considered important to confirm the rock layer surface during construction, and the quality assessments during piling becomes necessary. We believe that the piling data also improve the reliability of the retaining walls.

1.2 *Proposed method with piling data*

The rock layer with an SPT (Standard Penetration Test) N-value of 50 or more can be confirmed by seismic exploration and boring. However, the accuracy of the seismic exploration is estimated to be around 2 m (e.g. JGCA 2017) and it is difficult to carry out boreholes throughout the construction area. Borehole investigations are generally conducted every 30-300 m for road lines (Tony 2009). Therefore, it is difficult to determine accurately the depth of the rock layer surface all along the structures that have long horizontal sections such as a retaining wall, from the above-mentioned ground investigation alone.

Also, Ishihara et al. (2015) proposed a method of estimating geotechnical information from the piling data of the rotary press-in piling. This technique can estimate the boundaries of the rock layer with all piles.

This paper proposes the construction management system with the piling data (Figure 1). The depth of the rock layer surface is estimated from the piling data and compared with its design value determined from the preliminary ground investigations. If the estimated depth is deeper than the design value, the countermeasure is taken to extend the pile length. Otherwise, the pile length is maintained as designed. Compared with the measure that simply extending all piles, the proposed method is expected not to take unnecessary countermeasures.

In the observational method for the retaining construction, the prediction of the wall deformations and force are updated step by step, and the number of props can be controlled accordingly (e.g. Young & Ho 1994). In contrast, the proposed method is expected to give another approach as an observational method for the cantilever retaining wall.

DOI: 10.1201/9781003215226-29

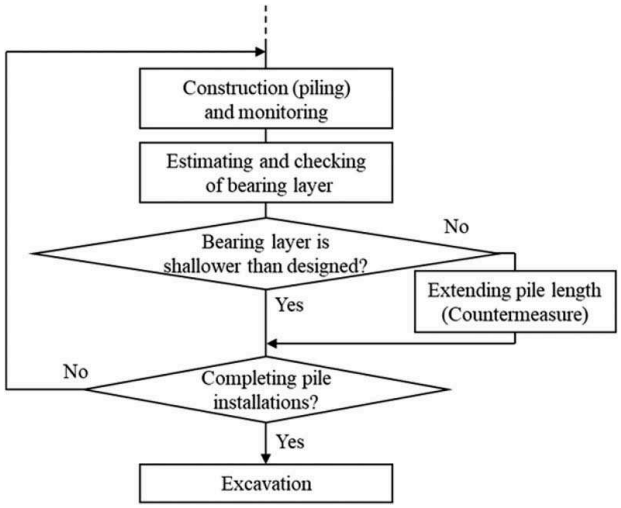

Figure 1. Procedure of construction management with piling data.

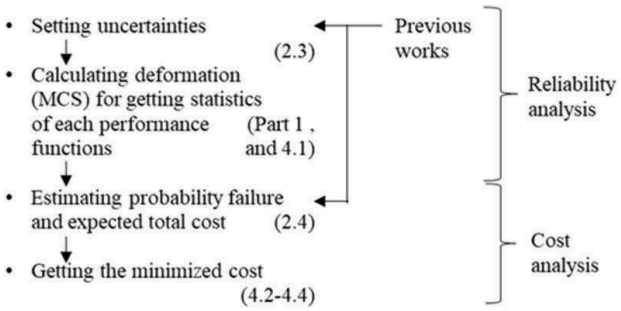

Figure 2. Flow of research steps.

1.3 *Objective*

This paper aims to study the cost effectiveness of the construction management using piling data for cantilever walls in stiff ground. A reliability analysis is conducted setting geotechnical uncertainties, including the depth of the stiff ground, as the random variable, X_i, to estimate probability failures. Then, a cost analysis is conducted to compare the expected total cost between the cases with and w/o the piling data (Figure 2).

2 METHOD

2.1 *Overview*

A reliability analysis was performed on a two-layer cantilever retaining wall (Figure 3), as in Part 1. The expected total cost was calculated based on Monte Carlo Simulation (MCS, e.g. Honjo 2008) and determine the optimized embedment depth.

This paper considered the rotational failure (Ultimate Limit State, ULS) and the deformation failure (Serviceability Limit State, SLS). This is because flexural failure seldom happens if the allowable displacement of the wall top, δ_a, is designed to be about 50 mm in the persistent design situation.

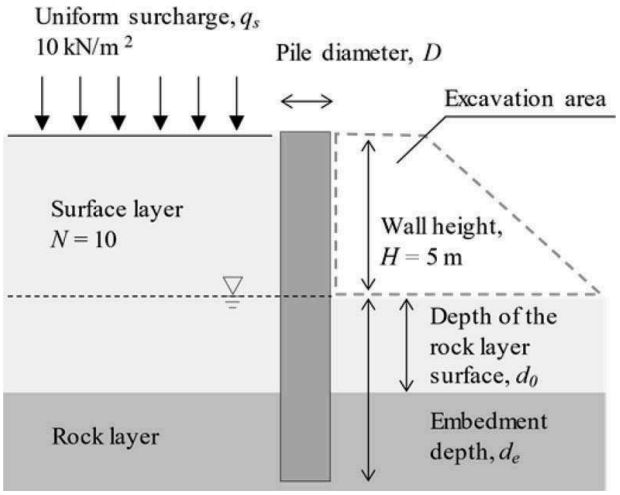

Figure 3. Illustrative analysis model of cantilever retaining wall.

$$Z_{d_e} = d_e - d_{eq}(X_i) \quad \text{(rotational failure)} \qquad (1)$$

$$Z_{\delta_{top}} = \delta_a - \delta_{top}(X_i) \quad \text{(deformation failure)} \qquad (2)$$

where d_e: embedment depth, d_{eq}: critical embedment depth for extreme equilibrium, δ_{top}: displacement of wall top.

2.2 *Analysis cases*

The cross sections of piles were determined so that the effect of the piling data can be large with reference to Part 1, and they were common in all cases; a pile diameter, D, was 1000 mm and a plate thickness was 10 mm; the N-value of the rock layer, N_r, was 1500; the depth of the rock layer surface, d_0, was 3.0 m; and stiffness factor $\Sigma\beta_i d_i$ was 1.5-5.0 (which corresponds to the embedment depth (d_e) of 4.1-9.7 m). The calculation method and other conditions followed Part 1.

Three cases were carried out: Case A as the standard: Case B with a large standard deviation (SD) of d_0: and Case C with a lower coefficient of variation (COV) of E_0 (Table 1) with reference to Phoon et al. 2016. This was because it is unlikely that d_0 is known in advance, and also because uniaxial compaction tests and in-situ horizontal loading are sometimes conducted in actual projects.

Table 1. Analysis cases.

Case	SD of d_0	COV of E_0	Piling data
A-1	0.5 m	1.2	Not utilized
A-2	0.5 m	1.2	Utilized
B-1	1.0 m	1.2	Not utilized
B-2	1.0 m	1.2	Utilized
C-1	0.5 m	0.4	Not utilized
C-2	0.5 m	0.4	Utilized

The reliability index and the expected total cost were calculated in each case, and the effect of the construction management (i.e. utilization of the piling data) on these values were examined.

The SD of d_0 in Case B, 1.0 m, was judged as realistic based on Ohki et al. (2004). It was for comparison with Case A. In Case C, the in-situ horizontal loading test was assumed to supply the mean value of the deformation coefficient, E_0, which was consistent with the predesigned of Case A.

Since there was no information on the estimation accuracy of the depth layer, it was assumed that the boundary could be estimated by the piling data with no error when the difference of N-value between the boundaries was large.

2.3 *Reliability analysis*

2.3.1 *Method*

MCS was performed 5000 times in each case to obtain the reliability index, β. Since it is difficult to obtain the probability of failure, P_f, directly from the MCS when P_f is smaller than 10^{-3} (the general target reliability index for ULS is from 3.1 to 4.3, ISO 2394), the following method was used. First, the mean and SD of each performance function, Z, were calculated by MCS, then the log-normal distribution was assumed. The conformity was confirmed by the Quantile-Quantile (Q-Q) Plot, which will be discussed later in Section 4.1. Finally, the reliability index was obtained by assuming the standard normal distribution.

$$P_f = \text{Prob}\,(Z<0) \tag{3}$$

$$\beta = -\Phi^{-1}(P_f) \tag{4}$$

where $\Phi(.)$ is the standard normal cumulative distribution function.

Since the reliability index increased monotonically with the embedment depth, it was linearly complemented between MCS results.

2.3.2 *Random variables and their correlations*

Part 2 assumed the correlation between the random variables for MCS setting 0.3 as poor correlation and 0.7 as high correlation with reference to Kulhawy & Mayne (1990), Ito & Kitahara (1985), Ogawa & Matsumoto (1978) (Table 2). The remaining statistics of the random variables (mean, coefficient of variation, and probability distribution) were the same as in Part 1.

2.4 *Cost analysis*

2.4.1 *Expected total cost*

The expected total cost, C_{tot} is sum of the building cost, C_b, and the maintenance cost, C_m, and the expected cost of the failure, C_f, which would be minimized for the optimal design (e.g. ISO 2394):

$$C_{tot} = C_b + C_m + P_f C_f \tag{5}$$

Since the cost for excavation (a part of C_b) and the maintenance cost were independent of the wall specification, these were omitted in this paper, and the simplified expected total cost C_{tot}^* was introduced as follows:

$$C_{tot}^* = C_p + P_c C_c + P_f C_f \tag{6}$$

where C_p is the piling cost, C_c is the countermeasure cost and P_c is the probability of the countermeasure.

2.4.2 *Piling cost*

Pile installation cost was estimated based on JPA (2019), which is a cost estimation standard of

Table 2. Correlation coefficients between variables.

X_i	N_s	γ_s	E_{0s}	$tan\phi_s$	N_r	γ_r	E_{0r}	$tan\phi_r$	c_r	d_0	q_s
N_s	1.0	0.0	0.0	0.0	0.0	0.0	0.0	0.0	0.0	0.0	0.0
γ_s		1.0	0.3	0.3	0.0	0.0	0.0	0.0	0.0	0.0	0.0
E_{0s}			1.0	0.7	0.0	0.0	0.0	0.0	0.0	0.0	0.0
$tan\phi_s$	Surface layer			1.0	0.0	0.0	0.0	0.0	0.0	0.0	0.0
N_r					1.0	0.0	0.0	0.0	0.0	0.0	0.0
γ_r						1.0	0.3	0.3	0.0	0.0	0.0
E_{0r}							1.0	0.7	0.0	0.0	0.0
$tan\phi_r$								1.0	-0.7	0.0	0.0
c_r					Rock layer				1.0	0.0	0.0
d_0		Symmetry								1.0	0.0
q_s											1.0

Note: Subscripts s and r represent surface layer and rock layer, respectively.

Press-in operation in Japan. Its outline in English has been shown in Suzuki & Kimura (2021). Also, in order to focus on the effect of construction data, steel pipe pile welding was not considered.

2.4.3 *Failure cost*

Failure cost includes function loss and fatalities as well as repair cost of structures (e.g. Kanda & Shaf 1997). It widely varies depending on the structural type, location, evaluation method of human life, etc. In this paper, the failure cost at the SLS was set to be 1.5 million Japanese Yen (JPY) per meter, with the reference to the subsidence repair of small-scale buildings due to liquefaction (such as underpinning or grout injection) (AIJ 2008).

On the other hand, the expected cost of failure at the ULS was assumed to be 30 times the piling cost so that the expected total cost was minimized with β=3.0, although the relationship between failure costs and construction costs varies depending on the structures and surroundings. Also, though failures at the SLS and ULS had a correlation, the probability of failure at these limit states were different by an order of magnitude, so the failure cost was considered separately at these two limit states.

2.4.4 *Countermeasure cost*

Assuming that the depth of the rock layer surface followed a normal distribution and the designed depth was its mean, the probability of countermeasure (P_c) became 50%. Figure 4 shows the pile extension length and its frequency, which is half-normal distribution. The mean length of the extension became about 0.8 times the SD of d_0.

The cost of countermeasures included the cost of the operations and the materials of the pile (instead of concrete cap), but not the time and cost for decision making on the implementation of the countermeasure.

Besides, Kakurai et al. (2006) stated that more than 2 m difference in pile length took a lot of time to repair a pile foundation. In the case of the cantilever retaining wall, we believe that the difference from the design can be absorbed by the concrete cap at the top of the pile after excavation, even if it is greater than 2 m.

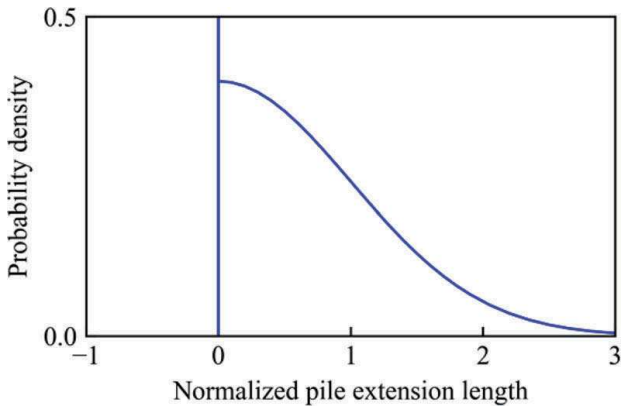

Figure 4. Distribution of the pile extension length normalized by the standard deviation of the depth of the rock layer surface.

3 EFFECT OF THE PILE EXTENTION AS COUNTERMEASURE AGAINST FAILURE

This chapter describes the effect of the countermeasures on preventing the deformation failure and rotational failure before the cost analysis in Section 4, and check the applicability of the countermeasure.

3.1 *Deformation failure (SLS)*

Figure 5 shows the relationship between the wall top displacement and the scatter of the depth of the rock layer surface, d_0, by MCS. When d_0 were less than the design value of 3.0 m, the countermeasures were not conducted, so the plots were omitted in the figure.

Without the piling data, the displacements were weakly correlated with d_0. Naturally, the variations in the same depth were due to variations of other variables such as the deformation coefficient, E_0.

On the other hand, with the piling data, the scatter of the displacement decreased. And the correlation between the displacement and d_0 became weaker.

3.2 *Rotational failure (ULS)*

Figure 6 shows the relationship between the critical embedment depth and the scatter of d_0. The dot line represents the boundary of the occurrence of the rotational failure.

The critical embedment depth and d_0 had a strong correlation. When the embedment depth was designed

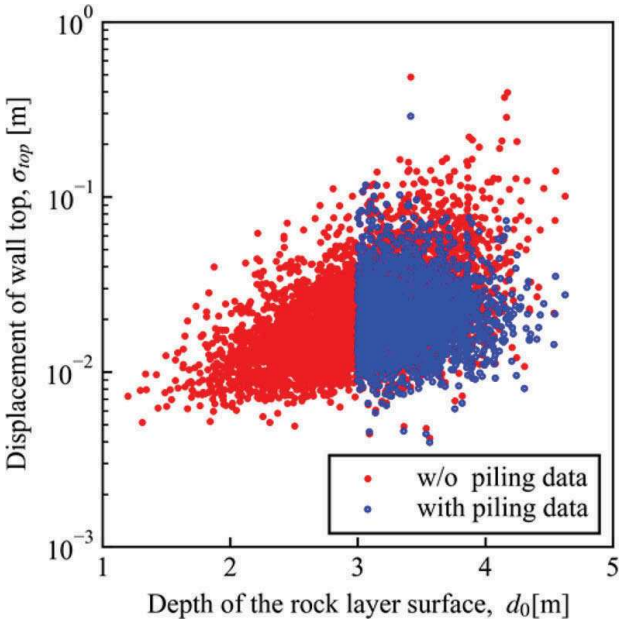

Figure 5. An example of the effect of countermeasures on the displacement of the wall top (Case A, d_e =4.9 m).

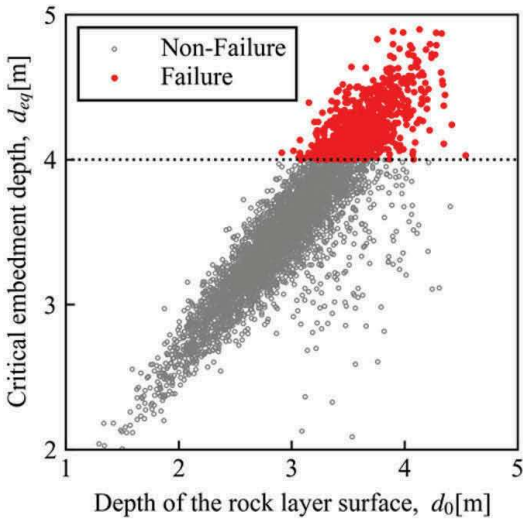

(a) without piling data (Case A-1)

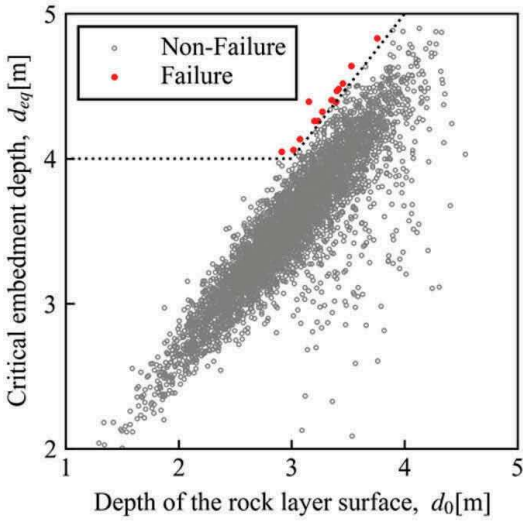

(b) with piling data (Case A-2)

Figure 6. Examples of rotational failure due to different construction managements (d_e =4.0 m).

to be 4.0 m for example, the probability of failure was about 17 % without the piling data (as shown in red dots of Figure 6a), but it became as small as 0.3 % with the piling data (Figure 6b).

The proposed method, i.e. the countermeasure against the scatter of the depth of the rock layer, was valid against the deformation failure and the rotational failure. It was also efficient, comparing with the countermeasure that simply extending the entire pile length.

4 RESULTS AND DISCUSSION ON THE RELIABILITY AND COST ANALYSIS

First, we confirm that the performance function calculated by MCS fit a lognormal probability density function. Then, we show the results of the cost analysis, and discuss the influence of the variation of d_0 and E_0 on the expected total cost.

4.1 *Probability density distribution*

Figure 7 shows an example of a histogram of the wall displacement and the critical embedment depth, a probability density assuming the lognormal distribution, and a Q-Q plot for the lognormal distribution.

Q-Q Plots showed that the MCS results were in good agreement with the log-normal distribution, although the log-normal distribution slightly overestimated the probability in the upper part. So, the assumption of the log-normal distribution was valid.

4.2 *Results of reliability index and expected total cost*

Figure 8 shows the relationship between the embedment depth and the reliability index and the expected total cost in Case A. The reliability index increased monotonically with the embedment depth for both construction managements (that is, with and w/o the piling data), and settled to a certain value (Figure 8a and c). This was because embedding more than a sufficient length did not affect the behavior of the cantilever wall retaining wall. The difference between the construction managements was larger at ULS than at SLS. This might be due to both the greater effect of pile embedment on rotational failure and the greater cost at the ultimate failure. In addition, since the reliability index converged at SLS, the piling data was not be useful when the embedment depth was long enough.

The costs were convex parabolic to the pile embedment, and the reliability index for SLS where the cost was minimized was about 1.5 (Figure 8a and b). Since 1.5 is the target value for SLS in ISO 2394, the subsidence repair cost assumed in Section 2.4 was generally reasonable. Also, most of the cost difference between cases with and w/o the piling data was the cost of countermeasures when the embedment depth was large.

Next, Figure 9 shows the reliability index and the expected total cost in Case B, with SD of d_0 of 1.0m. The reliability index increased monotonically and converged at enough embedment (Figure 9a and c), as in Case A, and the differences of the construction managements were larger in Case B than in Case A. And the convergent reliability index at SLS was less than in Case A. The reliability index for ULS also showed similar trend as Case A.

Finally, Figure 10 shows the results of Case C, where the uncertainty of E_0 is updated by the ground investigations. In both construction managements, the reliability indices were larger than that in Case A, and the slope of the reliability index were also

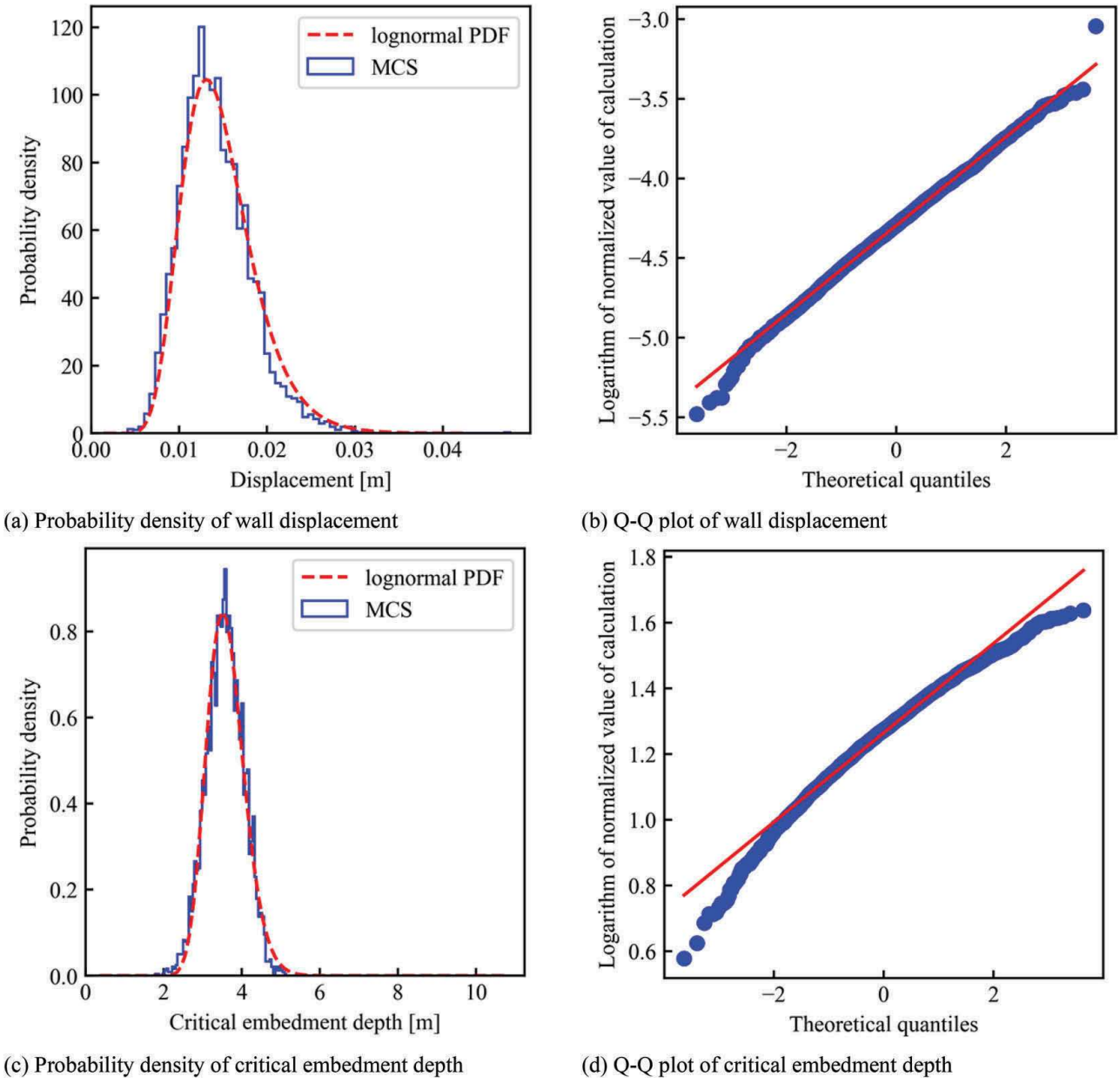

(a) Probability density of wall displacement

(b) Q-Q plot of wall displacement

(c) Probability density of critical embedment depth

(d) Q-Q plot of critical embedment depth

Figure 7. The probability density and lognormal distribution (d_e=4.9, Case A-1, without piling data) and its Q-Q plot.

larger than that in Case A. As a result, the minimum expected costs of both construction managements were smaller than those in Case A (Figure 8b).

4.3 *Influence of the scatters of the depth of the rock layer surface on expected total cost*

Table 3 summarizes the minimum expected total cost for each case normalized by the minimum expected total cost of Case A.

The differences of the expected total costs with and w/o the piling data were maximized in Case B both at SLS and ULS. The difference is about 8% at SLS and about 27% at ULS.

The minimum expected total cost of Case B-1 was 6% larger at SLS and 17% larger at ULS than those of Case A-1 respectively. On the other hand, those of Case B-2 was only 2% larger at SLS and 3% at ULS than those of Case A-2. So, the piling data enabled the cost to be stable regardless of the scatters of the depth of the rock layer surface, d_0.

In this paper, the scatter of d_0 was assumed to be constant and known before construction. However, it varies greatly in different regions and it is difficult to estimate qualitatively in advance from the ground investigation. Therefore, it is not practical to consider the depth variation of the rock layer in the preliminary design. It is advisable to use the piling data, especially when the inhomogeneity of the ground is foreseen but not qualitatively in advance.

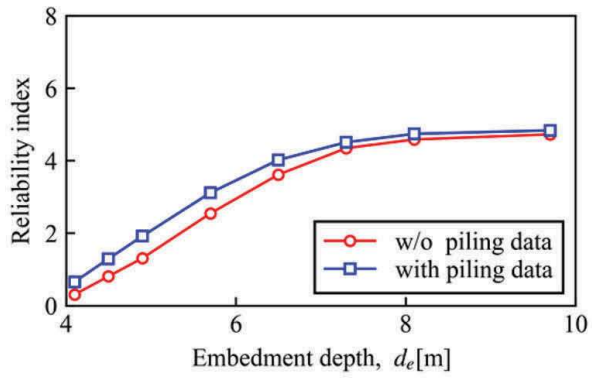

(a) Reliability index at SLS

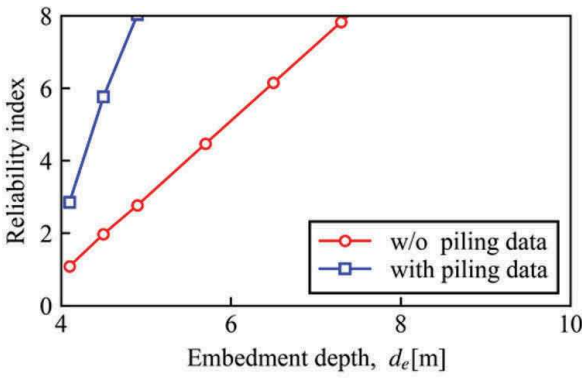

(c) Reliability index at ULS

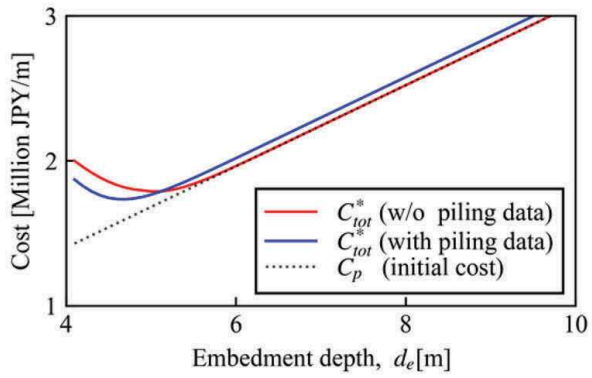

(b) Expected total cost at SLS

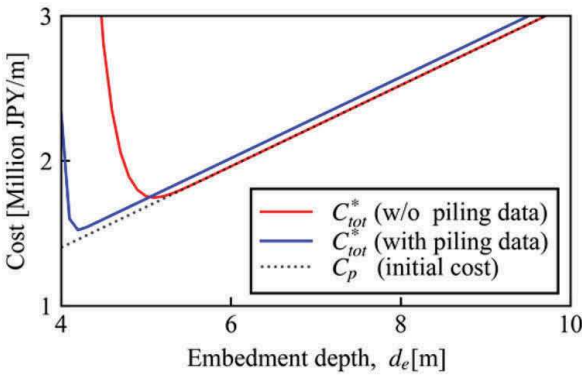

(d) Expected total cost at ULS

Figure 8. Analysis results of Case A.

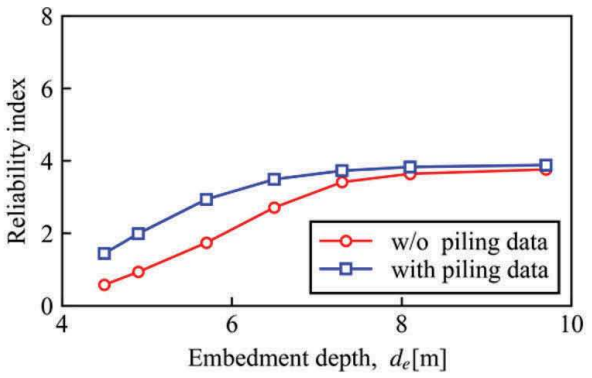

(a) Reliability index at SLS

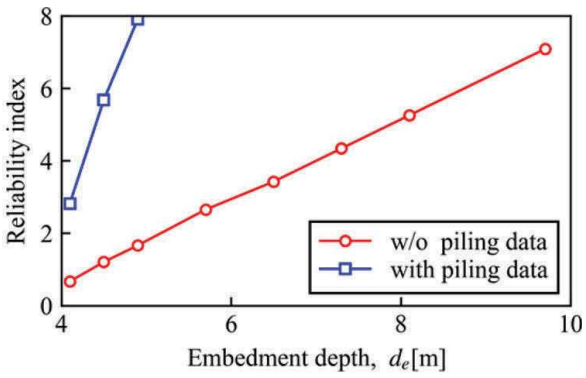

(c) Reliability index at ULS

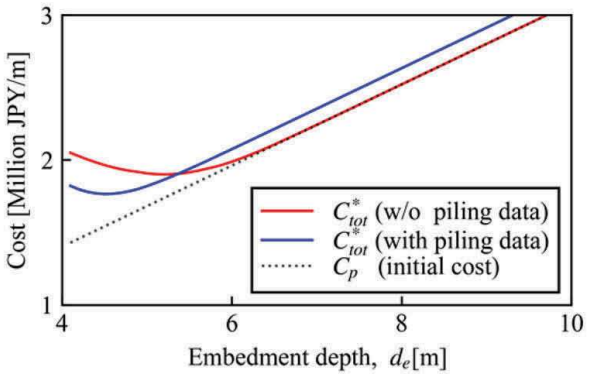

(b) Expected total cost at SLS

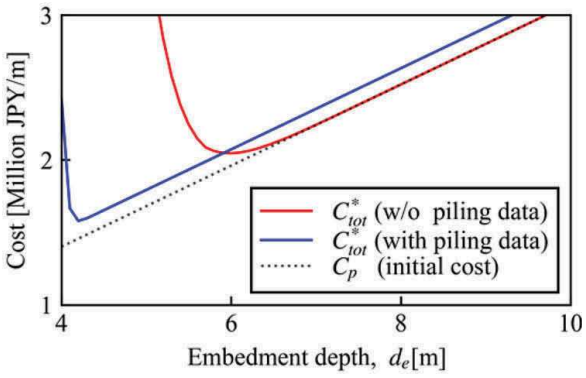

(d) Expected total cost at ULS

Figure 9. Analysis results of Case B.

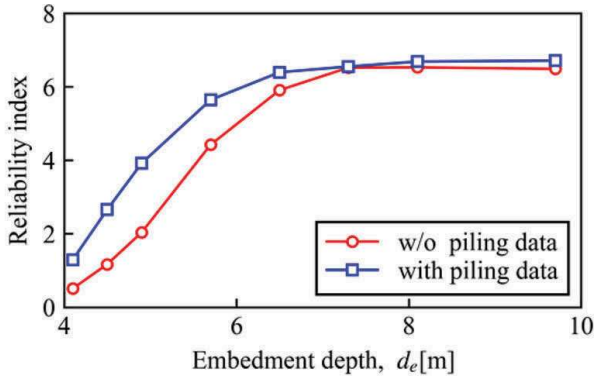

(a) Reliability index

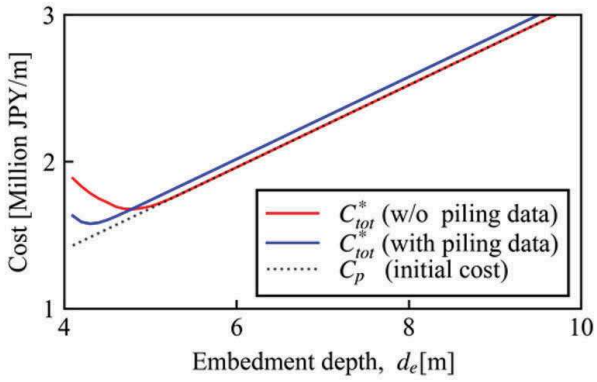

(b) Expected total cost

Figure 10. Analysis results of Case C at SLS.

Table 3. Normalized minimum expected total cost.

(a) Deformation failure (SLS)

	Case			diff. between	
	A	B	C	A & B	A & C
w/o PD.	1.00	1.06	0.94	0.06	0.06
with PD.	0.97	0.99	0.88	0.02	0.09
diff.	0.03	0.08	0.06		

(b) Rotational failure (ULS)

	A	B		diff. between A & B
w/o PD.	1.00	1.17	-	0.17
with PD.	0.87	0.90	-	0.03
diff.	0.13	0.27		

Note: PD. represents piling data.

4.4 *Influence of the geotechnical investigation on the expected total cost*

The difference of the costs with and w/o the piling data was larger in Case C than in Case A (Table 3). The piling data were effective also when geotechnical investigations were conducted.

5 CONCLUSIONS AND FUTURE ISSUES

This paper described a framework of the construction management using the piling data for the cantilever retaining wall, and assessed its effectiveness. The conclusions were summarized as follows;

- The scatter of the depth of the rock layer surface, d_0, was correlated with the displacement of the wall top and the critical embedment depth. The counter-measure to determine the extension of piles from the piling data was appropriate and effective.
- When the embedment depth was long enough, the proposed method could not prevent the SLS failure.
- The difference of the expected cost by the construction management was about 8% at SLS and 27% at ULS at most.
- Without the piling data, higher SD of d_0 increased the expected total cost. With piling data, on the other hand, it did not affect the cost much. Considering that the variation of d_0 is usually unknown, the proposed method can be practical.
- The piling data were effective to reduce the expected cost, even when geotechnical investigations were conducted.

Although this paper dealt with cantilever retaining walls, it can be expected that the proposed method is effective in avoiding the rotational failure of the propped or anchored walls as well.

Besides, the following issues are to be addressed in the future;

- Estimation accuracy In this paper, it was assumed that the rock layers could be reliably confirmed during construction, but verification of the estimation accuracy and its consideration are necessary.
- Use of estimated ground strength/stiffness
- In this paper, the piling data was used only to estimate the depth, but the estimation of the ground strength/stiffness from the piling data could also contribute to improving the reliability.

REFERENCES

Architectural Institute of Japan (AIJ). 2008. *Recommendations for Designing of Small Buildings Foundations*, Tokyo: AIJ (in Japanese).

Honjo, Y. 2008. Monte Carlo simulation in reliability analysis. *Reliability-based design in geotechnical engineering: computations and applications*: 169–191.

International Standard ISO/FDIN 2394. 1998. *General Principles on Reliability for Structures*, Zurich: ISO. Appendix E

Ishihara, Y. Stuart Haigh & Malcolm Bolton. 2015. Estimating base resistance and N value in rotary press-in, *Soils and Foundations*, Volume 55, Issue 4: 788–797.

Ito, H., & Kitahara, Y. 1985. The actual condition and some considerations about the scattering of the mechanical properties of a rock masses, *Report of Central Research Institute of Electric Power Industry (CRIEPI)*, No.384025. Tokyo: CRIEPI (in Japanese).

Japan Geotechnical Consultants Association (JGCA or ZENCHIREN). 2017. *(Draft) Report on the Investigation for Pile Foundations on Rock Layer.* (In Japanese) https://www.zenchiren.or.jp/geocenter/pdf/201701.pdf

Japan Press-in Association (JPA). 2019. *(Draft) Standard Cost Estimation Material: Gyropress Method – Steel tubular pile Press-in Method assisted by rotary cutting* (in Japanese).

Kakurai M., Tsujimoto, K., Kuwabara, F. & Manabe, M. 2009. Relationships soil exploration and pile construction (Part 1), *Summaries of technical papers of annual meeting 2009 of Architectural Institute of Japan (AIJ)*: 595–596. (in Japanese).

Kanda, J. and Shah, H. 1997. Engineering role in failure cost evaluation for buildings, *Structural Safety*, 19(1): 79–90.

Kulhawy, F. H., & Mayne, P. W. 1990. Manual on estimating soil properties for foundation design, *Electric Power Research Inst., EPRI-EL-6800*, Calif.: Palo Alto.

Ogawa, F. & Matsumoto, K. 1978. The Correlation of the Mechanical and Index Properties of Soils in Harbour Districts, *Report of the Port and Harbour Research Institute (PHRI)*, Vol.17, No.3, Tokyo: PHRI (in Japanese).

Ohki, H., Nagata, M., Saeki, E. & Kuwabara, H., 2005. Fluctuation on bearing strata levels of piles (part 2). *Proceedings of the 40th Technical Report of the Annual Meeting of the Japan Geotechnical Society, Japan*: 1549–1550 (in Japanese).

Phoon, K. K., W. A. Prakoso, Y. Wang, & J. Ching. 2016. Uncertainty Representation of Geotechnical Design Parameters. Chap. 3 in *Reliability of Geotechnical Structures in ISO2394*, Rotterdam: CRC Press: 49–87.

Suzuki N. & Kimura Y. 2021. Summary of case histories of retaining wall installed by rotary cutting press-in method, *Proceedings of the Second International Conference on Press-in Engineering 2021*, *Kochi* (under review).

Suzuki N., Nagai K. & Sanagawa T. 2021. Reliability analysis on cantilever retaining walls embedded into stiff ground (Part 1: contribution of major uncertainties in the elasto-plastic subgrade reaction method), *Proceedings of the Second International Conference on Press-in Engineering 2021*, *Kochi* (under review).

Tony Waltham. 2009. *Foundations of Engineering Geology*, Third Edition. Rotterdam: CRC Press: p.47.

Young, D. K., & Ho, E. W. L. 1994. The observational approach to design of a sheet-piled retaining wall. *Géotechnique*, 44(4): 637–654.

APPENDIX

Symbols and abbreviations used in the paper are as follows:

C_{tot}	JPY	:	Expected total cost
C_{tot}^*	JPY	:	Simplified expected total cost
C_f	JPY	:	Cost of failure
C_p	JPY	:	Cost of piling operation
C_c	JPY	:	Cost of countermeasure
D	m	:	Outer pile diameter
d_i	m	:	Depth of each layer
d_e	m	:	Embedment depth
d_{eq}	m	:	Critical embedment depth for extreme equilibrium
d_0	m	:	Depth of the stiff ground, or thickness of the surface layer
E_0	N/mm^2	:	Deformation coefficient of the ground (flat-plate loading test)
H	m	:	Height of structures, that is excavation depth
N	-	:	SPT N-value (blows per 300 mm penetration)
P_f	-	:	Probability of failure
P_c	-	:	Probability of countermeasure
q_s	kN/m^3	:	Any uniform surcharge at the ground surface
X_i	-	:	Random variable
Z	-	:	Performance function
$Z_{\delta top}$	-	:	Performance function on the deformation failure
Z_{de}	-	:	Performance function on the de rotational failure
β_i	m^{-1}	:	Stiffness factor of *i*-th ground layer
β	-	:	Reliability index
δ_{top}	m	:	Displacement of wall top
δ_a	m	:	Allowable displacement of wall

COV	:	Coefficient of Variation
MCS	:	Monte Carlo Simulation
PDF	:	Probability Density Function
SD	:	Standard Deviation
SLS	:	Serviceability Limit State
ULS	:	Ultimate Limit State